

UDC 666.266.6

*O.V. Savvova, O.V. Khrystych, D.A. Brazhnik, M.I. Timoshchuk, G.O. Brazhnik***ASSESSMENT OF THE CRYSTALLIZATION CAPACITY OF LITHIUM ALUMINOSILICATE GLASS-CERAMIC MATERIALS FOR ELECTRICAL APPLICATIONS****O.M. Beketov National University of Urban Economy in Kharkiv, Kharkiv, Ukraine**

The article analyzes the prospects of developing thermally and mechanically stable lithium aluminosilicate glass-ceramic materials for electrotechnical applications. The crystallization ability of lithium aluminosilicate glass-ceramics was thermodynamically forecasted by determining the interaction mechanisms of the solid phases of spodumene, eucryptite, and lithium disilicate through phase equilibrium calculations in the  $\text{Li}_2\text{O}-\text{Al}_2\text{O}_3-\text{SiO}_2$  system. Modified compositions of lithium-aluminosilicate glasses were obtained using glass-forming components ( $\text{B}_2\text{O}_3$ ,  $\text{P}_2\text{O}_5$ ,  $\text{Sb}_2\text{O}_3$ ), modifying components ( $\text{CaO}$ ,  $\text{SrO}$ ,  $\text{MgO}$ ,  $\text{BaO}$ ), and crystallization catalysts ( $\text{ZrO}_2$ ,  $\text{CeO}_2$ ,  $\text{TiO}_2$ ,  $\text{SnO}_2$ ,  $\text{ZnO}$ ). The influence of the chemical composition of the glasses on the sequential appearance of crystalline phases in solid solutions based on  $\beta$ -quartz and lithium metasilicate ( $T \approx 800-850$  K),  $\beta$ -eucryptite ( $T \approx 900$  K), and  $\beta$ -spodumene and lithium disilicate ( $T \approx 1000-1100$  K) was analyzed. In addition, the peculiarities of the mechanisms of structure and phase formation in experimental glasses during the preparation of glass-ceramic materials were determined, and optimal heat-treatment regimes were selected. The developed glass-ceramic materials are characterized by their high thermal and mechanical properties, making them promising candidates for use as high-strength substrates in electronic systems.

**Keywords:** glass-ceramic materials, lithium aluminosilicate glasses, eucryptite, spodumene, thermodynamic calculations, crystallization.

**DOI:** 10.32434/0321-4095-2026-164-1-4-14

**Introduction**

The design and organization of high-temperature technological processes in the modern ceramic, refractory and glass industries presents scientists and manufacturers with the important task of developing a correct model for assessing the formation of crystalline phases and their interaction, and achieving the desired physical, mechanical and technical properties of the material in a rational manner. The phase diagram of the  $\text{Li}_2\text{O}-\text{Al}_2\text{O}_3-\text{SiO}_2$  system forms the basis for developing ceramic, glass-ceramic and glass products containing eucryptite and/or spodumene

in their composition. The main feature of eucryptite and spodumene-containing compositions of materials is the low value of the thermal coefficient of linear expansion (TCLE) at temperatures up to 1473 K, which is characterized by high-temperature modifications of the eucryptite and spodumene phases and reaches values of about  $-90 \cdot 10^{-7} \text{ K}^{-1}$  and  $9 \cdot 10^{-7} \text{ K}^{-1}$ , respectively. Predicting the crystallization course of  $\beta$ -eucryptite and  $\beta$ -spodumene based on thermodynamic calculations, as well as evaluating the reproducibility of data in the practical implementation of technology for developing ceramic and glass-ceramic

© O.V. Savvova, O.V. Khrystych, D.A. Brazhnik, M.I. Timoshchuk, G.O. Brazhnik, 2026



This article is an open access article distributed under the terms and conditions of the Creative Commons Attribution (CC BY) license (<https://creativecommons.org/licenses/by/4.0/>).

*O.V. Savvova, O.V. Khrystych, D.A. Brazhnik, M.I. Timoshchuk, G.O. Brazhnik*

materials that can withstand significant thermal loads, is highly valuable. Considerable attention is currently being paid to processing transparent, nanostructured glass-ceramics, which are used in the development of compact electronic systems and have a low TCLE. The role of chemical components and additives, as well as the effect of heat treatment and microstructure evolution during processing, is also being considered [1].

Creating composites based on  $\beta$ -eucryptite and high-strength crystalline phases is an important scientific and practical way of obtaining ceramic materials that are simultaneously strong and heat-resistant. In particular, adding 30 wt.%  $\beta$ -eucryptite to cordierite ceramics and sintering them at 1573 K creates a composite material with high physical and mechanical properties and low crack resistance and thermal coefficient of linear expansion of  $-1.31 \cdot 10^{-6} \text{ K}^{-1}$  [2]. This composite material exhibits the TLCE values of  $-0.13 \cdot 10^{-6} \text{ K}^{-1}$  and a bending strength of 140 MPa. It contains 15.65 wt.% of submicron-sized aluminum nano-oxide grains (99.7% of the theoretical density), which are dispersed in a lithium aluminosilicate glass matrix. The difficulty of creating composites using  $\beta$ -eucryptite is associated with residual compression stresses on the grains of  $\beta$ -eucryptite due to the mismatch in TCLR between aluminum or zirconium oxide and  $\beta$ -eucryptite [3]. Increasing the sintering temperature to 1823 K and the nanosized  $\beta$ -eucryptite content to 30 wt.% decreases the apparent porosity of the aluminum oxide-based composite. These composites exhibit a CLTE of  $-1.036 \cdot 10^{-6} \text{ K}^{-1}$  and improved mechanical strength values [4].

Thermal incompatibility in composites can be overcome by creating composites based on  $\text{Al}_2\text{O}_3$  and  $\beta$ -eucryptite glass-ceramics in the form of ultrafine powders [5]. The formation of phases with different TCLE values in a multiphase ceramic material leads to thermal stresses and the possible formation of microcracks in the structure, contributing to energy dissipation when the material is operated at high temperatures. When designing such glass-ceramic materials (GCMs), it should be borne in mind that the glass phase has a higher thermal conductivity value than the crystalline compound and is more resistant to temperature changes. Using glass-ceramic materials reduces the thermal stress at the boundaries of  $\text{Al}_2\text{O}_3$  grains by increasing the TLCE of the lithium-alumina glass phase enveloping the grain. Geodakyan et al. [5] demonstrated that glass-ceramic materials based on  $\beta$ -eucryptite can be replaced with an equivalent amount of glass containing  $\text{Li}_2\text{O}-2\text{SiO}_2$  or a mixture of  $\text{Li}_2\text{CO}_3$  and  $\text{SiO}_2$  powders.

Using low-melting glass ( $T_{\text{melting}} \leq 1523 \text{ K}$ ) based on the  $\text{Li}_2\text{O}-\text{Al}_2\text{O}_3-\text{SiO}_2$  system could intensify the processes associated with the formation of the  $\beta$ -eucryptite crystal phase and the sintering of the ceramic material as a whole. The firing of eucryptite ceramics should be carried out at a temperature of 1623 K with an isothermal holding time of about 3 hours to form the structure of materials and achieve specified physical and technical properties ( $\sigma = 167 \text{ MPa}$ ,  $\text{TLCE}_{\alpha_{293-673}} = -13.1 \cdot 10^{-7} \text{ K}^{-1}$ , heat resistance of 1323 K,  $\varepsilon = 7.8$ ,  $\text{tg}\delta = 0.01$ ) [6]. However, the formation of the  $\beta$ -eucryptite phase, which is characterized by prismatic hexagonal crystals sized 4–7  $\mu\text{m}$ , is a significant factor contributing to the reduction of fracture toughness in the glass-composite eucryptite-containing materials. This reduces their service life, particularly when subjected to significant thermal and mechanical loads.

Improved thermomechanical properties can be achieved in products by creating solid-solution compounds (SCMs) that contain several crystalline phases. In particular, SCMs containing  $\beta$ -eucryptite and lithium phosphate [7] or  $\beta$ -eucryptite and celsian are characterized by enhanced mechanical properties. These materials exhibit high mechanical properties (bending strength of 88–126 MPa) and improved synthesis parameters ( $T_{\text{firing}} = 1223 \text{ K}$ ,  $\tau = 1 \text{ h}$ ) [8]. There are known GCMs with TLCE ranging from  $-5.91 \cdot 10^{-7} \text{ K}^{-1}$  to  $2.48 \cdot 10^{-7} \text{ K}^{-1}$  within the temperature ranges of 293–573 K and 300–737 K, respectively. These materials are also characterized by rapid phase transformations:  $\beta$ -eucryptite into  $\beta$ -spodumene and enstatite into clinoenstatite at 1123 K ( $\tau = 2 \text{ h}$ ) and 1223 K ( $\tau = 2 \text{ h}$ ), respectively [9]. However, high temperatures and considerable duration of the heat treatment process for lithium aluminosilicate-based GCMs not only reduce their manufacturability, but also significantly decrease their mechanical properties. For example, the flexural strength and fracture toughness values were 154 MPa and  $2.46 \text{ MPa}\cdot\text{m}^{1/2}$ , respectively [10], which can be explained by a decrease in crack resistance due to an increase in crystal size.

The key to creating high-strength eucryptite-spodumene solid-solution composite materials (GCMs) based on the  $\text{Li}_2\text{O}-\text{Al}_2\text{O}_3-\text{SiO}_2$  system is to study the formation processes of their structures under conditions of low-temperature, short-term heat treatment. This can be achieved through thermodynamic evaluation to predict the course of solid-phase interactions in eucryptite-spodumene compositions on the state diagram of the specified system, as well as through experimental determination of the effect of glass-forming and modifying

components on the nature of glass crystallization.

The aim of this work is to determine the chemistry of the solid-state interaction of spodumene and eucryptite by conducting thermodynamic calculations of the coexistence of single, double, and ternary phases of the  $\text{Li}_2\text{O}-\text{Al}_2\text{O}_3-\text{SiO}_2$  system. The influence of glass composition on the crystallization temperature range and sequential formation of intermediate final crystalline phases will also be established.

#### Methods and materials

The research methodology is based on utilizing the features of the phase diagrams of the  $\text{Li}_2\text{O}-\text{Al}_2\text{O}_3-\text{SiO}_2$  system, investigating the subsolidus phase coexistence region by means of thermodynamic analysis of phase interactions. This allows us to select optimal technological solutions to achieve the target phase composition of the glass-ceramic materials.

According to the phase diagram of the  $\text{Li}_2\text{O}-\text{Al}_2\text{O}_3-\text{SiO}_2$  system [11], the crystalline phases spodumene and eucryptite lie along the tie line connecting  $\text{SiO}_2$  and  $\text{Li}_2\text{O}\cdot\text{Al}_2\text{O}_3$  (Fig. 1). These phases are characterized by a series of metastable solid solutions of K-quartz type (whose end members include keatite and high-temperature spodumene) and O-quartz type (with  $\beta$ -quartz and  $\beta$ -eucryptite as the end members). As noted earlier in ref. [12], the crystallization of glasses leads to the appearance of unstable solid solutions with structures close to  $\beta$ -quartz. This indicates the necessity of analyzing the chemistry of solid-state reactions that may occur between the ternary compounds, eucryptite and spodumene, as well as their constituent binary phases within the  $\text{Li}_2\text{O}-\text{Al}_2\text{O}_3$  and  $\text{Li}_2\text{O}-\text{SiO}_2$  systems.

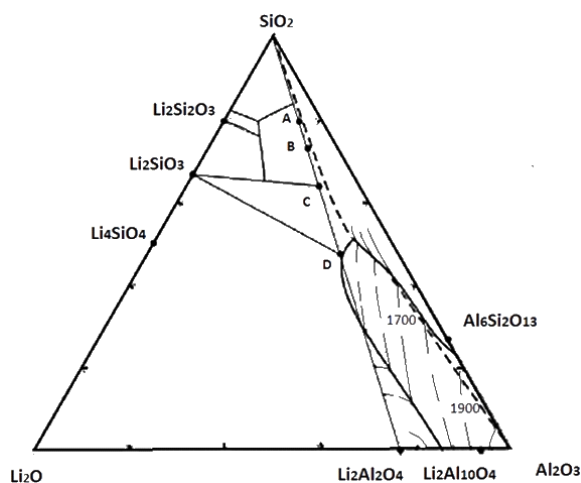


Fig. 1. Subsolidus structure of the  $\text{Li}_2\text{O}-\text{Al}_2\text{O}_3-\text{SiO}_2$  system:

A= $\text{Li}_2\text{O}\cdot\text{Al}_2\text{O}_3\cdot 8\text{SiO}_2$  ( $\text{LiAlSi}_4\text{O}_8$ ), B= $\text{Li}_2\text{O}\cdot\text{Al}_2\text{O}_3\cdot 6\text{SiO}_2$  ( $\text{LiAlSi}_3\text{O}_8$ ), C= $\text{Li}_2\text{O}\cdot\text{Al}_2\text{O}_3\cdot 4\text{SiO}_2$  ( $\text{LiAlSi}_2\text{O}_6$ ), D= $\text{Li}_2\text{O}\cdot\text{Al}_2\text{O}_3\cdot 2\text{SiO}_2$  ( $\text{LiAlSiO}_4$ )

Calculations were performed using standard data on exchange equilibria between lithium-containing aluminosilicates and alkali feldspars, as well as thermodynamic data for binary compounds [13]. The data presented in Table 1 were utilized to predict phase transformations within the subsolidus region of the  $\text{Li}_2\text{O}-\text{Al}_2\text{O}_3-\text{SiO}_2$  phase diagram.

The research methodology was based on the determination of isobaric-isothermal potentials without accounting for the temperature dependence of heat capacity, and without considering phase transitions between high- and low-temperature polymorphs of the corresponding phases.

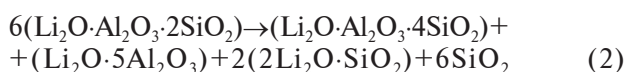
Experimental glass batches were melted in corundum crucibles using a laboratory electric furnace at temperatures ranging from 1673 to 1873 K, followed by casting the melt onto a metal plate.

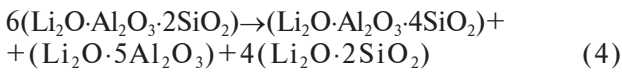
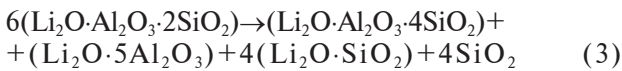
Thermogravimetric analysis was performed using a Q-1500D derivatograph from the Paulik-Paulik-Erdey system. X-ray phase analysis was conducted using a DRON-3M X-ray diffractometer. The crystallization ability was evaluated in a gradient furnace with a temperature range of 293–1173 K and current voltage of 0–170 V. Petrography analysis using an NU-2e optical microscope at magnifications ranging from 25 $\times$  to 1200 $\times$  in transmitted light was employed to determine the nature and amount of crystalline phases in the materials.

The thermal coefficient of linear expansion (TCLE) of the glasses was measured using a DKV-5A quartz dilatometer in accordance with ASTM C 372-94 (2007). Compressive strength was determined according to EN ISO 21690:2012(E).

#### Investigation of the subsolidus phase coexistence region in the $\text{Li}_2\text{O}-\text{Al}_2\text{O}_3-\text{SiO}_2$ system

As the compositional point of eucryptite lies outside the liquidus field and based on data from ref. [14] regarding the section of the system between eucryptite and silicon dioxide, the crystallization pathway of eucryptite was analyzed. According to ref. [14], the first phase to appear in the melt is spodumene. Subsequently, lithium pentaaluminat formation is expected, and crystallization continues up to 1673 K, at which point decomposition into a eucryptite-like substance and alumina occurs. Therefore, it was deemed reasonable to consider subsequent solid-state reactions (1)–(4) in which eucryptite acts as the initial compound:





It should be noted that the appearance of mullite ( $3\text{Al}_2\text{O}_3\cdot 2\text{SiO}_2$ ) or corundum/alumina in terms of chemical reactions of eucryptite decomposition into spodumene and lithium pentaaluminate ( $\text{Al}_2\text{O}_3$ ) is not expected due to the lack of Al atoms, which are necessarily taken into account in the above-mentioned final compounds.

*Investigation of the crystallization ability of glass-ceramic materials*

To investigate the phase formation mechanism in the  $\text{Li}_2\text{O}-\text{Al}_2\text{O}_3-\text{SiO}_2$  system, compositions from [12,15] were selected within the crystallization region of the eucryptite-spodumene solid solution, featuring a high  $\text{Al}_2\text{O}_3$  content (over 10 wt.%) and lithium disilicate (Table 2).

The requirements for the phase composition and structure of glass-ceramic materials were taken into account when selecting the following components for glass formation ( $\text{B}_2\text{O}_3$ ,  $\text{P}_2\text{O}_5$ ,  $\text{Sb}_2\text{O}_3$ ); for modification ( $\text{CaO}$ ,  $\text{SrO}$ ,  $\text{MgO}$ ,  $\text{ZnO}$ ,  $\text{BaO}$ ) and for crystallisation catalysts ( $\text{ZrO}_2$ ,  $\text{CeO}_2$ ,  $\text{TiO}_2$ ,  $\text{SnO}_2$ ):

- simultaneous crystallization of crystalline phases with high thermo-mechanical properties ( $\beta$ -eucryptite,  $\beta$ -spodumene, lithium disilicate);
- crystallization within the region of metastable liquid immiscibility with the formation of nuclei whose composition is close to that of the parent glass;
- formation of a bulk-crystallized structure at low temperatures (923–1123 K) within a short processing time ( $\approx 1-2$  h);
- development of an oriented nanostructure with translational crystal symmetry through directed dendritic crystallization;
- surface hardening occurs through the healing of cracks during surface crystallization and vitrification.

Table 1

Thermodynamic properties of the components of the  $\text{Li}_2\text{O}-\text{Al}_2\text{O}_3-\text{SiO}_2$  system

Phases	Compound	Enthalpy, kJ/mol	Entropy, J/mol·K
eucryptite	$\text{Li}_2\text{O}\cdot\text{Al}_2\text{O}_3\cdot 2\text{SiO}_2$	-2144.048	90.793
spodumene	$\text{Li}_2\text{O}\cdot\text{Al}_2\text{O}_3\cdot 4\text{SiO}_2$	-3053.500	131.210
lithium monoaluminate	$\text{Li}_2\text{O}\cdot\text{Al}_2\text{O}_3/\text{LiAlO}_2$	-1187.700	53.350
lithium pentaaluminate	$\text{Li}_2\text{O}\cdot 5\text{Al}_2\text{O}_3$	-9125.480	299.720
lithium orthosilicate	$2\text{Li}_2\text{O}\cdot\text{SiO}_2/\text{Li}_4\text{SiO}_4$	-2299.000	126.000
lithium disilicate	$\text{Li}_2\text{O}\cdot 2\text{SiO}_2/\text{Li}_2\text{Si}_2\text{O}_5$	-2584.900	123.500
lithium metasilicate	$\text{Li}_2\text{O}\cdot\text{SiO}_2/\text{Li}_2\text{SiO}_3$	-1669.500	81.300
lithium oxosilicate	$4\text{Li}_2\text{O}\cdot\text{SiO}_2/\text{Li}_8\text{SiO}_6$	-3527.000	170.000
$\beta$ -quartz	$\beta$ - $\text{SiO}_2$	-910.648	41.338

Table 2

Chemical composition, heat treatment method and characteristics of the crystalline phase of the developed compositions

Designation	Chemical composition, wt.%						Heat treatment mode	Type and content of the crystalline phase
	$\text{Li}_2\text{O}$	$\text{Al}_2\text{O}_3$	$\text{SiO}_2$	$\Sigma(\text{B}_2\text{O}_3, \text{P}_2\text{O}_5, \text{Sb}_2\text{O}_3)$	$\Sigma(\text{CaO}, \text{SrO}, \text{MgO}, \text{ZnO}, \text{BaO})$	$\Sigma(\text{ZrO}_2, \text{CeO}_2, \text{TiO}_2, \text{SnO}_2)$		
Opaque eucryptite-spodumene GCM SP-2M	11.0	10.5	68.5	4.2	4.0	4.0	I st. – T=923 K, $\tau=1$ h; II st. – T=1123 K, $\tau=1$ h	80 vol.% $\beta$ - $\text{LiAlSi}_2\text{O}_6$ and $\beta$ - $\text{LiAlSiO}_4$
Opaque spodumene GCM SP-10M	7.0	18.0	60.0	4.5	4.0	3.5	I st. – T=803 K, $\tau=1$ h; II st. – T=1073 K, $\tau=1$ h	80 vol.% $\beta$ - $\text{LiAlSi}_2\text{O}_6$
Optically transparent GCM based on lithium disilicate SL-12M	15.0	4.0	60.0	6.5	6.0	8.5	I st. – T=803 K, $\tau=1$ h; II st. – T=1073 K, $\tau=5$ min	50 vol.% $\text{Li}_2\text{Si}_2\text{O}_5$ and $\beta$ - $\text{LiAlSi}_2\text{O}_6$

## Results and discussion

### Thermodynamic calculations

All reactions are characterized by negative values of the isobaric-isothermal potential, which indicates their thermodynamic probability of occurrence, as illustrated in Fig. 2. It should be noted that reactions (1) to (3) proceed with the presence of  $\beta$ -quartz in the final compounds.

Reaction (1) is characterized by the highest value of the isobaric-isothermal potential up to 1104 K. At approximately 1104 K, according to ref. [13], a peritectic reaction occurs in which lithium metasilicate decomposes into lithium oxide and lithium orthosilicate.

Reaction (2) has the lowest thermodynamic probability at temperatures above 1200 K. The final products of this reaction are lithium orthosilicate, silicon dioxide, spodumene and lithium pentaaluminate.

Reaction (4) shows the lowest values of isobaric-isothermal potential; its products do not contain silicon dioxide, but in addition to spodumene and lithium pentaaluminate, lithium disilicate is also present.

According to ref. [13], during the structural formation of lithium-containing binary phases involving silicon oxide, it is thermodynamically plausible that the saturation of the binary compound, specifically lithium disilicate, with silicon oxide may occur without the formation of  $\beta$ -quartz. It has been determined that the thermodynamic probability of reactions (1) to (3) increases as the amount of silicon oxide in the form of a separate  $\beta$ -quartz phase in the final reaction products decreases.

The location of the spodumene and eucryptite compositional points between the lithium aluminate and silicon dioxide compositional points indicates the need to take into account the reactions that occur with the formation of  $\beta$ -quartz:

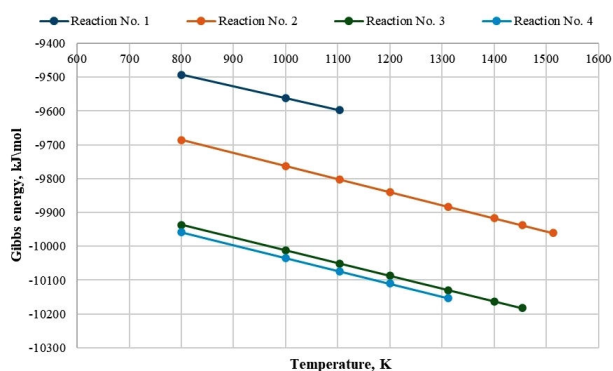


Fig. 2. Temperature dependence of the isobaric-isothermal potential of reactions (1), (2), (3) and (4)



The temperature dependence of changes in the isobaric-isothermal potential is presented in Table 3. Calculations were performed at temperatures of 800 and 1673 K.

The results of the isobaric-isothermal potential calculations for reactions (5) and (6) indicate their thermodynamic feasibility and demonstrate a higher thermodynamic probability for the decomposition of spodumene compared to eucryptite within the temperature range of 800–1673 K.

According to the results of thermodynamic analysis, it was determined that all reactions, except reaction (4), indicate the formation of  $\beta$ -quartz, which is consistent with the data on the presence of solid solutions of K-quartz and O-quartz, characteristic of spodumene and eucryptite. Therefore, it was found that all solid-phase reactions of eucryptite decomposition into spodumene, lithium pentaaluminate, and lithium silicates with silicon oxide are thermodynamically probable.

Notably, the most thermodynamically favorable reaction yields a final composition containing lithium disilicate and no free silicon oxide. This indicates a thermodynamic preference for the saturation of lithium disilicate with silicon oxide during its structural formation. The formation of  $\beta$ -quartz is associated with a decrease in thermodynamic probability via direct solid-state reactions, with its content in the final products increasing with temperature. Additionally, it was found that the simultaneous formation of  $\beta$ -quartz and lithium monoaluminate is thermodynamically probable during the solid-state decomposition of eucryptite and spodumene.

### Structure and phase formation processes in the experimental materials

The study of the crystallization mechanism revealed that all experimental glasses undergo bulk crystallization, leading to the formation of a glass-ceramic (sitalized) structure under low-temperature treatment conditions. This is confirmed by the presence of sharp exothermic peaks at 1073–1123 K, as illustrated in Fig. 3.

Table 3  
Dependence of changes in isobaric-isothermal potential

Reaction No.	Change in isobaric-isothermal potential, kJ/g-atom		
	$\Delta G = \Delta H^0 - T\Delta S$	T=800 K	T=1673 K
5	$-61.782 - 0.00323T$	-64.366	-67.186
6	$-88.839 - 0.00437T$	-92.335	-96.150

The experimental glasses exhibit the following crystallization behavior. In the first stage, intensive nucleation of lithium metasilicate and subsequent crystal growth occur near the softening temperature. This appears as an endothermic effect on thermograms at  $T=823\text{--}873\text{ K}$  (Fig. 3). This mechanism can be explained by the fact that diffusion processes, on which the equilibrium state formation rate directly depends, are significantly slowed down at low temperatures. This particularly affects the coordinated diffusion of  $\text{Al}^{3+}$  and  $\text{Li}^+$  ions. Consequently, aluminum atoms do not participate in the formation of stable phases at low temperatures, resulting in the formation of lithium metasilicate, a stable crystalline phase in contrast to lithium disilicate. This process is intensified by the lower viscosity of the lithium metasilicate phase, making its formation energetically favorable. Such a mechanism is most pronounced in the GCM composition SL-12M, which contains the lowest amount of alumina ( $\text{Al}_2\text{O}_3$ ).

For the lithium aluminosilicate glasses SP-2M and SP-10M, nucleation is predominantly characterized by the formation of  $\beta$ -quartz solid solutions, which have a higher viscosity than lithium metasilicate. Under these conditions, a significant number of nuclei form, creating favorable conditions for the subsequent development of  $\beta$ -eucryptite, which has a structure closely related to that of  $\beta$ -quartz.

A characteristic feature of the experimental GCMs is the occurrence of metastable liquid–liquid

phase separation, observed in the softening temperature range of  $823\text{--}873\text{ K}$ . This manifests as slight deviations on the thermogram curve and is confirmed by gradient thermal analysis (GTA) through the visualization of an opalescent structure that precedes surface crystallization (Fig. 4). This mechanism results in nanostructuring both at the surface and within the bulk of the GCMs during heat treatment and contributes to the healing of microcracks, which are potentially critical factors for structural failure under load. An important factor in the formation of crack-resistant nanostructures is the suppression of spherulite growth through phase separation of the glass, which is evidenced by the persistence of the opalescent structure in SP-10M and SL-12M glasses within the specified temperature range (Fig. 4).

In the second stage, the temperature rises to  $923\text{--}1023\text{ K}$  for SP-10M and SP-2M glasses containing more than 10 wt.%  $\text{Al}_2\text{O}_3$ . Due to the decreased viscosity of the glass and the easier diffusion of lithium and aluminum ions, the  $\beta$ -eucryptite solid solution crystallizes. This is formed by replacing some silicon atoms in the structure of high-temperature quartz with aluminum atoms paired with lithium atoms.

The crystallization intensity of SP-2M glass, characterized by an intense exo-effect peak at  $923\text{ K}$ , shifts to the low-temperature region due to an increase in lithium oxide content to 11 wt.% and a decrease in aluminum oxide content compared to SP-10M glass, for which the exo-effect is only recorded at  $973\text{ K}$  (Fig. 3). The elevated  $\text{Al}_2\text{O}_3$  content (18 wt %) and a significant amount of a combined crystallization catalyst  $\Sigma(\text{ZrO}_2, \text{CeO}_2, \text{TiO}_2, \text{SnO}_2)=4.0\text{ wt.}\%$  in the SP-10M glass enable the formation of up to 40 vol.% of crystalline phases during low-temperature treatment. The development of the low-temperature  $\beta$ -eucryptite crystalline phase, chemically and structurally most similar to the glass matrix, allows for stress relaxation during thermal treatment, improving the integrity and stability of the material.

In the third stage, within the temperature range of  $1023\text{--}1123\text{ K}$ , experimental glasses SP-10M and SP-2M undergo recrystallization of metastable  $\beta$ -eucryptite crystals into stable  $\beta$ -spodumene crystals ( $\text{Li}_2\text{O}\cdot\text{Al}_2\text{O}_3\cdot 2\text{SiO}_2 \rightarrow \text{Li}_2\text{O}\cdot\text{Al}_2\text{O}_3\cdot 4\text{SiO}_2$ ) due to the incorporation of additional  $\text{SiO}_2$ . As a result of the more intensive crystallization in SP-10M during the second stage compared to SP-2M (Fig. 3), the quantity of orthorhombic  $\beta$ -spodumene is significant and reaches approximately 80 vol.% (Fig. 4). In SP-2M glass, the recrystallization process is incomplete, resulting in the formation of approximately 30 vol.%  $\beta$ -eucryptite and 50 vol.%  $\beta$ -spodumene. In the case of SL-12M glass, a minor exothermic effect at

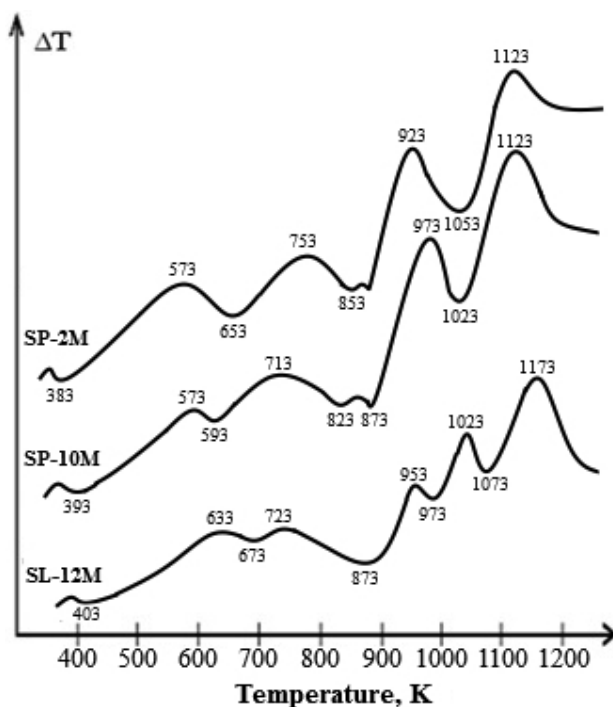


Fig. 3. Glass thermograms according to DTA data

1023 K indicates a limited amount of  $\beta$ -spodumene and concurrent recrystallization of lithium metasilicate into stable lithium disilicate crystals ( $T \approx 1073$  K), as recorded on DTA curves as exothermic peaks (Figs. 3 and 4).

It is important to note that in these glasses, crystallization occurs predominantly in the  $\beta$ -form of both eucryptite and spodumene, which possess lower free energy (thermodynamic potential) compared to their  $\alpha$ -counterparts that typically crystallize under specialized hydrothermal conditions. In the  $\beta$ -forms, aluminum enters the anionic framework in tetrahedral coordination with oxygen, just as it does in the glass network. Therefore, within the defined compositional ranges, the glasses exhibit a  $\beta$ -eucryptite-type short-range order, which leads to the nucleation of this phase.

These phases form through kinetic pathway with minimal energy barriers, as the hexagonal lattice symmetry of  $\beta$ -eucryptite is more compatible with the local structure of the amorphous glass. The  $\beta$ -eucryptite lattice adopts a high-temperature  $\beta$ -quartz-type structure, in which every second  $\text{Si}^{4+}$  ion layer is substituted by  $\text{Al}^{3+}$  and  $\text{Li}^+$ . This process is most pronounced in SP-2M and SP-10M compositions. A distinguishing feature of SP-2M glass is the accelerated surface crystallization driven by phase separation at lower temperatures. This promotes the formation of a

well-defined and intense  $\beta$ -eucryptite peak at 923 K (Fig. 5a), followed by its partial recrystallization into  $\beta$ -spodumene (Fig. 5b).

The results of the study of the crystallization ability of lithium aluminosilicate glasses containing glass-forming components ( $\text{B}_2\text{O}_3$ ,  $\text{P}_2\text{O}_5$ ,  $\text{Sb}_2\text{O}_3$ ) and modifying components ( $\text{CaO}$ ,  $\text{SrO}$ ,  $\text{MgO}$ ,  $\text{BaO}$ ), as well as crystallization catalysts ( $\text{ZrO}_2$ ,  $\text{CeO}_2$ ,  $\text{TiO}_2$ ,  $\text{SnO}_2$  and  $\text{ZnO}$ ) enable us to make the following statements about the mechanism of glass crystallization and the thermodynamic assessment of sub-solidus phase coexistence in the  $\text{Li}_2\text{O}-\text{Al}_2\text{O}_3-\text{SiO}_2$  system:

1. The thermodynamic probability of the course of reactions at the first stage is realized in glasses during heat treatment in the temperature range of 800 K and manifests itself as the formation of nuclei during the structure formation of silicon-containing phases: lithium metasilicate or solid solutions with the structure of  $\beta$ -quartz;

2. The structure of lithium aluminosilicate glasses during heat treatment is characterized by a series of metastable solid solutions of O-quartz with members of the  $\beta$ -quartz series, lithium metasilicate ( $T \approx 800-850$  K),  $\beta$ -eucryptite ( $T \approx 900$  K) and their recrystallization into stable crystalline phases of  $\beta$ -spodumene and lithium disilicate ( $T \approx 1000-1100$  K);

3. The influence of modifying components in the composition of lithium aluminosilicate glasses is

T, K	Marking		
	SP-2M	SP-10M	SL-12M
823			
873			
923			
973			
1023			
1073			
1123			
1173			

– opalescence of glass; – surface crystallization;  
 – bulk crystallization, with a crystalline phase content of 20 vol. %;  
 – bulk crystallization, 30 vol. %; – bulk crystallization, 40 vol. %;  
 – bulk crystallization, 50 vol. %; – bulk crystallization, 60 vol. %

Fig. 4. Crystallization ability of test glasses according to GTA data

manifested in ensuring phase separation with subsequent nucleation in the low-temperature region and nanostructuring ( $P_2O_5$ ,  $ZnO$ ,  $CeO_2$ ), viscosity regulation ( $SiO_2$ ,  $B_2O_3$ ,  $P_2O_5$ ,  $Sb_2O_3$ ,  $CaO$ ,  $SrO$ ,  $MgO$ ,  $BaO$ ) for the priority of the appearance of the first crystalline phase (solid solutions with a  $\beta$ -quartz structure for crystallization of  $\beta$ -spodumene and metasilicate for lithium disilicate) and intensification of crystallization ( $ZrO_2$ ,  $TiO_2$ ,  $SnO_2$ ) in a short time;

4. The probability of bulk crystallization of lithium aluminosilicate glasses under conditions of reduced temperatures with the presence of crystalline phases of 80 vol.%  $\beta$ - $LiAlSi_2O_6$  and  $\beta$ - $LiAlSiO_4$  or 80 vol.%  $\beta$ - $LiAlSi_2O_6$  or 50 vol.%  $Li_2Si_2O_5$  and  $\beta$ - $LiAlSi_2O_6$  to allow adjustment of thermo-mechanical properties according to the intended use of the materials.

The investigation of mechanical and thermal properties has shown that the compressive strength of the modified GCMs increases in comparison with the reference GCMs [12,15], reaching 720 MPa,

780 MPa, and 700 MPa for compositions SP-2M, SP-10M and SL-12M, respectively.

At the same time, the TCLE decreases in the following order: SP-2M > SP-10M > SL-12M, with corresponding values of  $15.4 \cdot 10^{-7} K^{-1}$ ,  $18.7 \cdot 10^{-7} K^{-1}$  and  $57.1 \cdot 10^{-7} K^{-1}$ , respectively. These properties confirm the high potential of these materials for use in the development of glass-ceramic systems intended for electrotechnical applications.

### Conclusions

The prospects of developing GCMs with simultaneously enhanced mechanical properties and improved thermal stability for electrotechnical applications were analyzed, and the feasibility of their synthesis based on the crystalline phases,  $\beta$ -eucryptite,  $\beta$ -spodumene, and lithium disilicate was determined.

The solid-state chemical interaction between  $\beta$ -spodumene and  $\beta$ -eucryptite was established through thermodynamic calculations of the coexistence of unary, binary, and ternary phases in the  $Li_2O$ - $Al_2O_3$ - $SiO_2$  system. Initial glass compositions

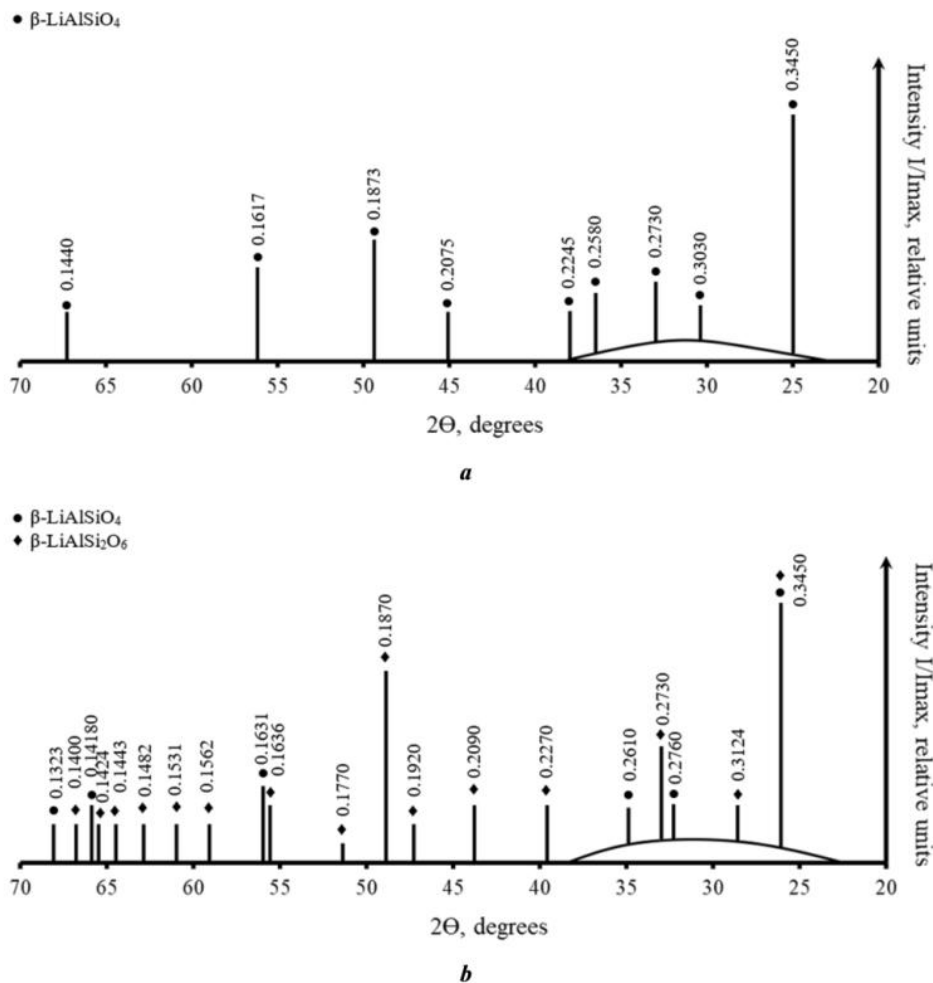


Fig. 5. X-ray diffraction patterns of experimental glass SP-2M

were selected and modified to ensure the crystallization of the high-strength  $\beta$ -spodumene,  $\beta$ -eucryptite and lithium disilicate phases. The peculiarities of the structure and phase formation processes were determined in the developed glasses under conditions of low-temperature, short-term heat treatment. At a temperature of 823–873 K, there was intensive formation of lithium metasilicate germs and growth of  $\beta$ -quartz solid solution germs near the softening temperature due to detestable liquation. This provides the prerequisites for the formation of  $\beta$ -eucryptite with a structure close to  $\beta$ -quartz. At temperatures between 923 and 1023 K,  $\beta$ -eucryptite solid solutions crystallize in glasses with a high  $\text{Al}_2\text{O}_3$  content (10 wt.%), by reducing the glass viscosity and facilitating the diffusion of lithium and aluminum ions. In the temperature range of 1023–1123 K, recrystallization of detestable  $\beta$ -eucryptite crystals occurs to form stable  $\beta$ -spodumene crystals (in glasses with an  $\text{Al}_2\text{O}_3$  content of 10 wt.%), and lithium metasilicate recrystallizes to form stable lithium disilicate crystals (in glasses with an  $\text{Al}_2\text{O}_3$  content of 4 wt.%).

The glass-ceramic materials developed by a two-stage low-temperature heat treatment are characterized by high thermal ( $\text{TLCE}=(15.4-57.1)\cdot 10^{-7} \text{ K}^{-1}$ ) and mechanical properties ( $\sigma=700-780 \text{ MPa}$ ) and can be recommended for use in the development of high-strength substrate materials for electronic systems.

## REFERENCES

1. Venkateswaran C., Sreemoolanadhan H., Vaish R. Lithium aluminosilicate (LAS) glass-ceramics: a review of recent progress // *Int. Mater. Rev.* – 2022. – Vol.67. – No. 6. – P.620-657.
2. The effect of  $\beta$ -eucryptite on cordierite ceramic materials prepared using a temperature-induced forming technique / Khattab R.M., Sadek H.E.H., Ajiba N.A., Badr H.A., Abo-Elmaged H.H. // *J. Eur. Ceram. Soc.* – 2023. – Vol.43. – No. 5. – P.2253-2268.
3. Thermal expansion of  $\beta$ -eucryptite in oxide-based ceramic composites / Pelletant A., Reveron H., Chevalier J., Fantozzi G., Guinot F., Blanchard L., et al. // *J. Eur. Ceram. Soc.* – 2013. – Vol.33. – No. 3. – P.531-538.
4. The effect of temperature on synthetic nano  $\beta$ -eucryptite and alumina ceramic materials: thermal expansion, mechanical, and physical properties / Abo almagad H.H., Hegazy W.H., Sebak M.E.M., Khattab R.M. // *Silicon.* – 2023. – Vol.15. – P.839-853.
5. The influence of beta-eucryptite glassceramics on the structure and main properties of alumina ceramics / Geodakyan J.A., Kostanyan A.K., Geodakyan K.J., Sagatelyan S.T., Petrosyan B.V. // 28th International Conference on Advanced Ceramics and Composites B: Ceramic Engineering and Science Proceedings. 2004. – Vol.25. – P.37-42.
6. Heat-resistant ceramics of  $\beta$ -eucryptite composition: peculiarities of production, microstructure and properties / Zaichuk A.V., Amelina A.A., Khomenko Y.S., Baskevich A.S., Kalishenko Y.R. // *Voprosy Khimii i Khimicheskoi Tekhnologii.* – 2020. – No. 2. – P.52-59.
7. Ion-exchange induced mechanical properties enhancement and microstructural modifications of transparent lithium aluminosilicate glass-ceramics / Mu Y., Qiu J., Wu L., Tian X., Wang J., Li L., et al. // *Ceram. Int.* – 2024. – Vol.50. – No. 9. – Part A. – P.14878-14883.
8. Khater G.A., Idris M. Preparation and properties of  $\text{Li}_2\text{O}-\text{BaO}-\text{Al}_2\text{O}_3-\text{SiO}_2$  glass-ceramic materials // *Process. Appl. Ceram.* – 2014. – Vol.8. – No. 4. – P.203-210.
9. Khater G.A., Morsi M.M. Glass-ceramics based on spodumene–enstatite system from natural raw materials // *Thermochim. Acta.* – 2011. – Vol.519. – No. 1-2. – P.6-11.
10. Mechanical and thermal expansion properties of  $\beta$ -eucryptite prepared by sol–gel methods and hot pressing / Xia L., Wen G.W., Qin C.L., Wang X.Y., Song L. // *Mater. Des.* – 2011. – Vol.32. – No. 5. – P.2526-2531.
11. Waetzig K., Hutzler T., Zschippang E. Materials for improved lifetime of saggar in production of Li-ion cathode powders // *Int. J. Appl. Ceram. Technol.* – 2025. – Vol.22. – No. 1. – Art. No. e14897.
12. High-strength spodumene glass-ceramic materials / Savvova O.V., Babich O.V., Voronov G.K., Ryabinin S.O. // *Strength Mater.* – 2017. – Vol.49. – No. 3. – P.479-486.
13. de Abreu D.A., Fabrichnaya O. Critical experiments and thermodynamic modeling of the  $\text{Li}_2\text{O}-\text{SiO}_2$  system // *Solids.* – 2024. – Vol.5. – P.303-320.
14. Thermochemistry of stuffed quartz-derivative phases along the join  $\text{LiAlSiO}_4-\text{SiO}_2$  / Xu H., Heaney P.J., Navrotsky A., Topor L., Liu J. // *Am. Mineral.* – 1999. – Vol.84. – No. 9. – P.1360-1369.
15. Investigation of structure formation in lithium silicate glasses on initial stages of nucleation / Savvova O., Babich O., Kuriakin M., Gritsova A., Topchiy V. // *Funct. Mater.* – 2017. – Vol.24. – No. 2. – P.311-317.

Received 18.07.2025

Revised 20.10.2025

Accepted 02.12.2025

Published 25.02.2026

**ОЦІНЮВАННЯ КРИСТАЛІЗАЦІЙНОЇ ЗДАТНОСТІ ЛІТІЙ-АЛЮМОСИЛІКАТНИХ СКЛОКЕРАМІЧНИХ МАТЕРІАЛІВ ДЛЯ ЕЛЕКТРОТЕХНІЧНОГО ВИКОРИСТАННЯ**

*О.В. Саввова, О.В. Христич, Д.А. Бражнік, М.І. Тимошук, Г.О. Бражнік*

В статті проаналізовано перспективність створення термічно- та механічностійких літій-алюмосилікатних скло-керамічних матеріалів для електротехнічного використання. Проведено термодинамічне прогнозування кристалізаційної здатності літій-алюмосилікатних склокерамічних матеріалів шляхом встановлення хімізму твердофазової взаємодії сподумену евкриптиту та дисилікату літію шляхом термодинамічних розрахунків співіснування фаз системи  $\text{Li}_2\text{O}-\text{Al}_2\text{O}_3-\text{SiO}_2$ . Модифіковано склади літій-алюмосилікатних стекел склоутворюючими ( $\text{B}_2\text{O}_3$ ,  $\text{P}_2\text{O}_5$ ,  $\text{Sb}_2\text{O}_3$ ) і модифікуючими ( $\text{CaO}$ ,  $\text{SrO}$ ,  $\text{MgO}$ ,  $\text{BaO}$ ) компонентами та каталізаторами кристалізації ( $\text{ZrO}_2$ ,  $\text{CeO}_2$ ,  $\text{TiO}_2$ ,  $\text{SnO}_2$ ,  $\text{ZnO}$ ) та одержано стекла. Проаналізовано вплив хімічного складу стекел на послідовній появи кристалічних фаз твердих розчинів на основі  $\beta$ -кварцу, метасилікату літію ( $T \approx 800-850$  K),  $\beta$ -евкриптиту ( $T \approx 900$  K) та  $\beta$ -сподумену, дисилікату літію ( $T \approx 1000-1100$  K) та визначено особливості механізму структуро- та фазоутворення у дослідних стеклах при одержанні склокристалічних матеріалів та обрано режими їх термічного оброблення. Розроблені склокерамічні характеризуються високими термічними та механічними властивостями та є перспективними при розробці матеріалів як високоміцних підкладок для електронних систем.

**Ключові слова:** склокерамічні матеріали, літій-алюмосилікатні стекла, евкриптит, сподумен, термодинамічні розрахунки, кристалізація.

**ASSESSMENT OF THE CRYSTALLIZATION CAPACITY OF LITHIUM ALUMINOSILICATE GLASS-CERAMIC MATERIALS FOR ELECTRICAL APPLICATIONS**

*O.V. Savvova\*, O.V. Khrystych, D.A. Brazhnik, M.I. Timoshchuk, G.O. Brazhnik*

**O.M. Beketov National University of Urban Economy in Kharkiv, Kharkiv, Ukraine**

\* e-mail: savvova\_oksana@ukr.net

The article analyzes the prospects of developing thermally and mechanically stable lithium aluminosilicate glass-ceramic materials for electrotechnical applications. The crystallization ability of lithium aluminosilicate glass-ceramics was thermodynamically forecasted by determining the interaction mechanisms of the solid phases of spodumene, eucryptite, and lithium disilicate through phase equilibrium calculations in the  $\text{Li}_2\text{O}-\text{Al}_2\text{O}_3-\text{SiO}_2$  system. Modified compositions of lithium-aluminosilicate glasses were obtained using glass-forming components ( $\text{B}_2\text{O}_3$ ,  $\text{P}_2\text{O}_5$ ,  $\text{Sb}_2\text{O}_3$ ), modifying components ( $\text{CaO}$ ,  $\text{SrO}$ ,  $\text{MgO}$ ,  $\text{BaO}$ ), and crystallization catalysts ( $\text{ZrO}_2$ ,  $\text{CeO}_2$ ,  $\text{TiO}_2$ ,  $\text{SnO}_2$ ,  $\text{ZnO}$ ). The influence of the chemical composition of the glasses on the sequential appearance of crystalline phases in solid solutions based on  $\beta$ -quartz and lithium metasilicate ( $T \approx 800-850$  K),  $\beta$ -eucryptite ( $T \approx 900$  K), and  $\beta$ -spodumene and lithium disilicate ( $T \approx 1000-1100$  K) was analyzed. In addition, the peculiarities of the mechanisms of structure and phase formation in experimental glasses during the preparation of glass-ceramic materials were determined, and optimal heat-treatment regimes were selected. The developed glass-ceramic materials are characterized by their high thermal and mechanical properties, making them promising candidates for use as high-strength substrates in electronic systems.

**Keywords:** glass-ceramic materials; lithium aluminosilicate glasses; eucryptite; spodumene; thermodynamic calculations; crystallization.

**REFERENCES**

1. Venkateswaran C, Sreemoolanadhan H, Vaish R. Lithium aluminosilicate (LAS) glass-ceramics: a review of recent progress. *Int Mater Rev.* 2022; 67(6): 620-657. doi: 10.1080/09506608.2021.1994108.
2. Khattab RM, Sadek HEH, Ajiba NA, Badr HA, Abo-almaged HH. The effect of  $\beta$ -eucryptite on cordierite ceramic materials prepared using a temperature-induced forming technique. *J Eur Ceram Soc.* 2023; 43: 2253-2268. doi: 10.1016/j.jeurceramsoc.2022.12.036.
3. Pelletant A, Reveron H, Chevalier J, Fantozzi G, Guinot F, Blanchard L, et al. Thermal expansion of  $\beta$ -eucryptite in oxide-based ceramic composites. *J Eur Ceram Soc.* 2013; 33: 531-538. doi: 10.1016/j.jeurceramsoc.2012.09.022.
4. Abo-almaged HH, Hegazy WH, Sebak MEM, Khattab RM. The effect of temperature on synthetic nano  $\beta$ -eucryptite and alumina ceramic materials: thermal expansion, mechanical, and physical properties. *Silicon.* 2023; 15: 839-853. doi: 10.1007/s12633-022-02049-z.
5. Geodakyan JA, Kostanyan AK, Geodakyan KJ, Sagatelyan ST, Petrosyan BV. The influence of beta-eucryptite glassceramics on the structure and main properties of alumina ceramics. In: Lara-Curzio E, Readey MJ, editors. *28th International Conference on Advanced Ceramics and Composites B: Ceramic Engineering and Science Proceedings, Volume 25.* 2004. p. 37-42. doi: 10.1002/9780470291191.ch7.

6. Zaichuk AV, Amelina AA, Khomenko YS, Baskevich AS, Kalishenko YR. Heat-resistant ceramics of  $\beta$ -eucryptite composition: peculiarities of production, microstructure and properties. *Voprosy Khimii i Khimicheskoi Tekhnologii*. 2020; (2): 52-59. doi: 10.32434/0321-4095-2020-129-2-52-59.

7. Mu Y, Qiu J, Wu L, Tian X, Wang J, Li L, et al. Ion-exchange induced mechanical properties enhancement and microstructural modifications of transparent lithium aluminosilicate glass-ceramics. *Ceram Int*. 2024; 50: 14878-14883. doi: 10.1016/j.ceramint.2024.01.403.

8. Khater GA, Idris MH. Preparation and properties of  $\text{Li}_2\text{O}$ - $\text{BaO}$ - $\text{Al}_2\text{O}_3$ - $\text{SiO}_2$  glass-ceramic materials. *Process Appl Ceram*. 2014; 8(4): 203-210. doi: 10.2298/PAC1404203K.

9. Khater GA, Morsi MM. Glass-ceramics based on spodumene-enstatite system from natural raw materials. *Thermochim Acta*. 2011; 519: 6-11. doi: 10.1016/j.tca.2011.02.021.

10. Xia L, Wen GW, Qin CL, Wang XY, Song L. Mechanical and thermal expansion properties of  $\beta$ -eucryptite prepared by sol-gel methods and hot pressing. *Mater Des*. 2011; 32: 2526-2531. doi: 10.1016/j.matdes.2011.01.054.

11. Waetzig K, Hutzler T, Zschippang E. Materials for improved lifetime of saggars in production of Li-ion cathode powders. *Int J Appl Ceram Technol*. 2025; 22: e14897. doi: 10.1111/ijac.14897.

12. Savvova OV, Babich OV, Voronov GK, Ryabinin SO. High-strength spodumene glass-ceramic materials. *Strength Mater*. 2017; 49: 479-486. doi: 10.1007/s11223-017-9890-4.

13. de Abreu DA, Fabrichnaya O. Critical experiments and thermodynamic modeling of the  $\text{Li}_2\text{O}$ - $\text{SiO}_2$  system. *Solids*. 2024; 5: 303-320. doi: 10.3390/solids5020020.

14. Xu H, Heaney PJ, Navrotsky A, Topor L, Liu J. Thermochemistry of stuffed quartz-derivative phases along the join  $\text{LiAlSiO}_4$ - $\text{SiO}_2$ . *Am Mineral*. 1999; 84(9): 1360-1369. doi: 10.2138/am-1999-0913.

15. Savvova O, Babich O, Kuriakin M, Grivtsova A, Topchiy V. Investigation of structure formation in lithium silicate glasses on initial stages of nucleation. *Funct Mater*. 2017; 24(2): 311-317. doi: 10.15407/fm24.02.311.